Optical and Quantum Electronics (2019) 51:311
https://doi.org/10.1007/s11082-019-2028-0

Locally resonant phononic crystals band-gap analysis on a two dimensional phononic crystal with a square and a triangular lattice

Khouloud Sellami[1] · **Hassiba Ketata**[1] · **Mohamed Hedi Ben Ghozlen**[1]

Received: 12 December 2018 / Accepted: 3 September 2019 / Published online: 11 September 2019

Abstract
Locally resonant phononic crystals (LRPC) are a new type of sound insulating material. Using the plane wave expansion method based on the Bloch theorem, we compute the band structure of two dimensional (2D) phononic crystals (PC) with square and triangular lattices. Such PC typically consists of infinitely long carbon rods coated with silicon rubber and embedded in an elastic background. Computational results show that gaps appear at the lower frequency range, which are lower than those expected from the Bragg mechanism. Those gaps are generated due to local resonances; the optimum gap is obtained by tuning the thickness ratio of the coating layer. The gap created by the LRPC depends on the filling fraction of the coating cylinders.

Keywords Phononic crystal · PWE · Bessel function · Complete band gap · Two dimensional LRPC · Triangular and square lattices · Bragg mechanism

1 Introduction

Phononic crystals (Khelif and Adibi 2015) are composite materials made up of a periodic distribution of inclusion in a matrix. As they are periodic structures, these materials may have, under some conditions, absolute acoustic band gaps (Khelif et al. 2010). In the frequency range of the gap, an incident wave will be reflected by the phononic crystal that operates then as a perfect non-absorbing mirror. Such a property is promising for a variety application, such as the reflection of seismic waves, the creation of acoustic shields or the construction of non-absorbent mirrors allowing insulation of phonic cavities. Recently, research on phononic crystals has experienced a serious advancement, in particular, through the development of theoretical calculation methods and tools for digital simulation. The existence of an absolute gap (Li et al. 2018) has been theoretically predicted (Kushwaha 1999; Sigalas and Economou 1993) before being experimentally demonstrated in a wide variety of phononic crystals (Pennec et al. 2010) consisting of solid (Vasseur

✉ Khouloud Sellami
sallamikhouloud@gmail.com

[1] Laboratory of Materials Physics, Faculty of Sciences of Sfax, BP 1171, 3000 Sfax, Tunisia

et al. 1998), or solid and fluid components (De Espinosa et al. 1998). It has been shown that the existence and the width of the absolute band prohibitions depend on the nature of the constituents, the contrast between the physical parameters (elastic densities and constants) of the inclusions and the matrix, the geometry of the inclusion, the shape of the inclusions and the filling factor. Therefore, for the creation of band gaps at low frequencies (Jiang et al. 2018), structures having small dimensions relative to the correspondent's wavelength is required. This objective has become possible, with the local resonance mechanism (LR) introduced for the first time by Liu et al (2000). Contrary to Bragg's mechanisms (Bria et al. 2011), the creation of a phononic gap by the localized resonance mechanism doesn't depend on the PC periodicity and the symmetry. Khelif et al (2010), studied theoretically the behavior of locally acoustic resonances of a periodic array of cylindrical pillars deposited on a semi-infinite substrate. Moreover, Achaoui et al (2011), found that the low frequency band gap arises because of a local resonance in phononic crystal of pillars.

In this paper the PC model and the plane wave expansion method (PWE) are described, position and width of Bragg gap are discussed. Then we present a new combination of materials to have locally resonant phonon crystals (LRPC). They consist of an epoxy matrix and implantation formed by two or three coaxial cylinders, it's about a heavy core (carbon) coated by a first layer of polymer (silicone rubber) then a second layer of carbon. The implantations are distributed over two types of crystal lattice, square and triangular. The overall implantation factor is fixed and the study is done on the contribution of the polymer layer to the presence of the gap associated with the locally resonance. Larabi et al (2007), studied locally resonant phononic crystals, band gap in multicoaxial cylindrical inclusions using the finite difference time domain method. Contrasted to the previous 2D PC model, our modified PWE method is the first used to calculate band structure of 2D multi-coaxial PC .Our current model has many advantages over the old model it's simpler, easier to fabricate and most important, it comes at a lower cost. All those are advantageous prospects within the practical applications.

2 Plane wave expansion method

2.1 Introduction to the method

The plane wave expansion method is widely used by the scientific community working in the fields of photonics and phononics, where the systems studied are usually periodic. One of its first applications was to obtain the states of electronic energy in the periodic metallic crystals (Herring 1940). Then it was widely used in photonic crystals (Plihal and Maradudin 1991; Meade et al. 1992) then in phononic crystals for the calculation of band structures. During the last few decades, the PWE has largely shown its effectiveness in the calculation of phononic band structures for different types of systems: Two-dimensional solid composite structures (Kushwaha et al. 1993; Vasseur et al. 1994) or solid-air (Sigalas and Economou 1996), in a one or two dimensional PC, Lamb waves propagating in plates (Hou and Assouar 2009; Sigalas and Economou 1994), in systems having one or more defects (Huang and Wu 2005; Sigalas 1997) as well as wave guiding in finite systems (Vasseur et al. 2008).

2.2 Formulation of the method

The study of elastic wave propagation in a homogeneous material is based on the fundamental principle of dynamics and Hooke's law which give us the equation of motion:

$$\rho \frac{\partial^2 u_i}{\partial t^2} = \frac{\partial^2 \left(c_{ijkl}\, u_k\right)}{\partial x_j \partial x_l} \tag{1}$$

Since the elastic constants c_{ijkl} and the density ρ are functions of the position $\vec{r}$, the components of the displacement vector $\vec{u}$ must verify the equation:

$$\rho(\vec{r}) \frac{\partial^2 u_i(\vec{r},t)}{\partial t^2} = \frac{\partial}{\partial x_j}(c_{ijkl}(\vec{r}) \frac{\partial u_k(\vec{r},t)}{\partial x_l}) \tag{2}$$

Using the Fourier series, $\rho(\vec{r})$ and $c_{ijkl}(\vec{r})$ can be expanded as,

$$\rho(\vec{r}) = \sum_{\vec{G}} R^{\vec{G}} \exp(j\vec{G}.\vec{r}) \quad c_{ijkl}(\vec{r}) = \sum_{\vec{G}} C_{ijkl}^{\vec{G}} \exp(j\vec{G}.\vec{r}) \tag{3}$$

where $\vec{G}$ is a vector of the reciprocal lattice and $\vec{r}(x_1, x_2, x_3)$,(x_3 is equivalent to z) is the position, and $C_{ijkl}^{\vec{G}}$ and $R^{\vec{G}}$ are the Fourier coefficients associated to the $\vec{G}$ vector. According to Bloch's theorem each wave propagating in a periodic phononic material is the product of a plane wave and a periodic function. Thus, the components of the displacement field $\vec{u}$, using Bloch's theorem, at the instant t and the position $\vec{r}$ are written below:

$$u_i(\vec{r},t) = e^{-j\omega t} \sum_{\vec{G}'} U_i^{\vec{k}+\vec{G}'} e^{j(\vec{k}+\vec{G}').\vec{r}} \tag{4}$$

$U_i^{\vec{k}+\vec{G}'}$ represents the amplitude of the harmonic associated to the $(\vec{k}+\vec{G}')$ vector of the reciprocal lattice with $\vec{k} = \left(k_1, k_2, k_3\right)$ as the Bloch wave vector belonging to the first Brillouin zone.

2.3 Development of motion equations for a bidirectional PC

Equation (1) can be rewritten finally as an eigenvalue problem:

$$\omega^2 \sum_{\vec{G}'} R^{\vec{G}-\vec{G}'} U_i^{\vec{k}+\vec{G}'} = \sum_{\vec{G}'} \sum_{\vec{G}} C_{ijkl}^{\vec{G}-\vec{G}'} (\vec{k}+\vec{G}')_j (\vec{k}+\vec{G})_l U_k^{\vec{k}+\vec{G}'}. \tag{5}$$

We represent the Fourier coefficient $C_{ijkl}^{\vec{G}}$ and $R^{\vec{G}}$ by the function

$$F(G) = \frac{1}{s} \int_S f(\vec{r}) \cdot e^{-iG\cdot r} dr, \tag{6}$$

where the integration is performed over the area of one lattice unit cell, and S is the area.

We choose the rods to have circular cross sections of radius R, then by integrating in Eq. (6),

$$\text{we} \quad \text{get: } F(G) = F_m \delta(G) + (F_i - F_m) \cdot 2f \frac{J_1(GR)}{(GR)}, \tag{7}$$

where J_1 is the Bessel function (Zhang et al. 2003) of the first kind of order I.

$$\delta(G) = \begin{cases} 1 \; G = 0 \\ 0 \; G \neq 0 \end{cases} \Rightarrow F(G) = \begin{cases} F_m + \left(F_i - F_m\right) \cdot f & G = 0 \\ \left(F_i - F_m\right) S(G) & G \neq 0 \end{cases} \tag{8}$$

In order to coat multilayer material on carbon rods, we evaluate F(G) according to

$$\begin{aligned} F(G) &= \left(F_m - F_{coat}\right) \cdot \left(f_1 - f_2\right) - \left(F_m - F_i\right) \cdot f_1 \; G = 0 \\ F(G) &= \left(F_m - F_{coat}\right) \cdot \left(2f_1 \tfrac{J_1(1,G.R)}{(1,G.R)} - 2f_2 \tfrac{J_1(1,G \cdot r_{coat})}{(1,G \cdot r_{coat})}\right) - \left(F_m - F_i\right) \cdot 2f_1 \tfrac{J_1(1,G \cdot r_{coat})}{(1,G \cdot r_{coat})} \quad G \neq 0 \end{aligned} \tag{9}$$

where r_{coat} and F_{coat} are respectively the radius and the filling fraction of the coated layer .

$\delta(G)$ is the Kronecker symbol coefficient and f is the filling factor defined as a fraction of the area occupied by the rods in a one-unit cell.With F_i and F_m referring to the acoustic constants (ρ and c_{ijkl}) for the rods and background separately, and f is the filling factor defined as the fraction of the area occupied by the rods in one unit cell. The factor S(G) relies on only one geometry of the rods and the lattice structures and it is given by the integration carried out over the area occupied by the rods in the unit cell. We name S(G) as the structure factor, and it is given by:

$$S(G) = \frac{1}{s} \int_{S_r} e^{-iG \cdot r} dr. \tag{10}$$

Where the integration is performed over the area (Sr) occupied by the rods in the unit cell.

According to Bloch theorem each characteristic of waves propagating in a periodic material is the product of a plane wave and a periodic function. Thus, the components of the displacement field $\vec{u}$, at the time t and the position $\vec{r}$ are written below:

$$u_i(\vec{r}, t) = e^{-j\omega t} \sum_{\vec{G}'} U_i^{\vec{k}+\vec{G}'} e^{j(\vec{k}+\vec{G}') \cdot \vec{r}} \tag{11}$$

ω is the pulsation, $U_i^{\vec{k}+\vec{G}'}$ represents the amplitude of the harmonic associated to the $(\vec{k}+\vec{G}')$ vector with $\vec{k} = \left(k_1, k_2, k_3\right)$ is the Bloch wave vector belonging to the first Brillouin zone.

By substituting all equations in Eq. (1) we obtained an eigenvalue problem for the eigenvectors $U^{\vec{k}+\vec{G}'}$ and the eigenfrequencies ω(k).

$$\omega^2 U^{\vec{k}+\vec{G}'} = (B^{\vec{G},\vec{G}'}) U^{\vec{k}+\vec{G}'} \tag{12}$$

$(B^{\vec{G},\vec{G}'})$ is an (3n, 3n) matrix, n is the number of vector $\vec{G}\vec{G}$(and $\vec{G}'\vec{G}'\vec{G}'\vec{G}'\vec{G}'\vec{G}'$) used in the summation (Eq. 10).

By letting $\vec{k}$ scan the area of the irreducible region of the Brillouin zone, the band structure is obtained.

2.4 Application for square and triangular lattice

Now we apply the above formulas to study explicitly the band structure of our model.

The plane wave expansion method is used to find the band structure and the computation is done with MATLAB, using 1369 plane waves to get accurate results. Such a PC is composed of a periodic array of infinite-length carbon cylinders embedded periodically in an epoxy resin background. The calculation is done on the three principal directions ΓM, ΓX and XM of the first Brillion zone of square and triangular lattice. This PC is presented

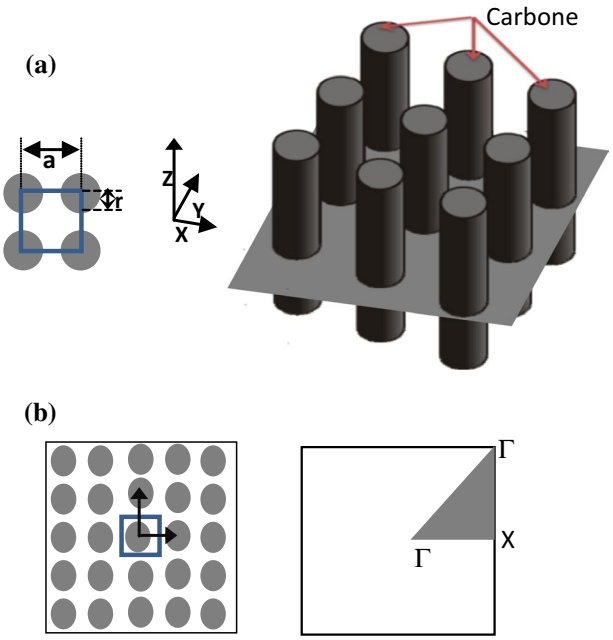

Fig. 1 **a** Two dimensional square phononic crystal of circular rods of radius r with lattice constant **a**. **b** The unit cell, basis lattice vectors and first Brillouin zone

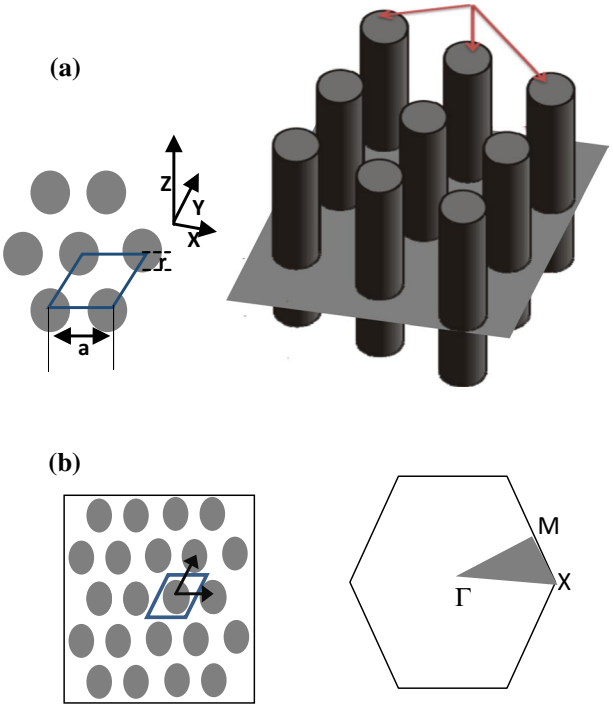

Fig. 2 **a** Two dimensional square phononic crystal of circular rods of radius r with lattice constant **a**. **b** The unit cell, basis lattice vectors and first Brillouin zone

for the two lattices in Figs. 1 and 2 with an infinite cylinder of carbon (Table 1) along the Z direction embedded in a periodic medium of epoxy resin along the plan (xy).First, we arranged the rods of radius r in a two dimensional square background with a lattice constant a, and basis vectors $(1,0,0)a$ and $(0,1,0)a$ of the first Brillion zone are shown respectively in Fig. 1a and in Fig. 1b. Then, we arranged the rods of radius r in a two dimensional triangular background with a lattice constant a, and basis vectors $(1,0,0)a$ and $\left(\frac{1}{2},\frac{\sqrt{3}}{2},0\right)a$ the first Brillion zone are shown respectively in Fig. 2a and in Fig. 2b.

3 Results

3.1 Bragg gap

Band structures of both square and triangular distributions are presented in (Fig. 4) and (Fig. 6), for the same lattice parameter a = 3 mm and the same filing fraction equal to 0.72.

3.1.1 Square lattice

To validate the PWE method for square lattice used in this paper, the band-gap structure of three-component phononic crystals considered by Zhang et al. (2003) is compared to results obtained by our written MATLAB program.

(Figure 3 shows a good agreement between results obtained by our MATLAB program and results obtained by the PWE method in the literature (Zhang et al. 2003).

We can notice in (Fig. 4), 4 absolute gaps in the frequency range 0.9 MHz $< f_q <$ 1.58 MHz, the largest gap appears between the 6th and the 7th bands with a width of $\Delta f_q = 0.07$ MHz.

The lower and upper edges are 1.11 MHz and 1.27 MHz, its gap-midgap ratio is $\Delta f_q / f_{qg} = 0.1280$.

3.1.2 Triangular lattice

We compared the band gap obtained by our triangular MATLAB codes with the band gap obtained by Pennec et al. (2010) (Fig. 5) and the obtained result shows a good agreement with their experimental result (we used the same materials and parameters in the published paper) :

Table 1 Mass density ρ, elastic constants C_{11}, C_{44} and C_{12} of epoxy, carbon and silicon rubber; $c_l = \sqrt{\frac{c_{11}}{\rho}}$, $c_t = \sqrt{\frac{c_{44}}{\rho}}$ represent respectively longitudinal and transverse speed of sound

Material	ρ (kg/m^3)	C_{11} (Pa)	C_{44} (Pa)	C_{12} (Pa)	C_l (m/s)	C_t (m/s)
Epoxy	1200	9.6107×10^9	1.6147×10^9	6.3813×10^9	2830	1160
Carbon	1800	3.06×10^{11}	1.3×10^{11}	8.8×10^{10}	13,038	6992.1
Silicon (Larabi et al. 2007)	1300	748,800	46,800	655,200	24	6

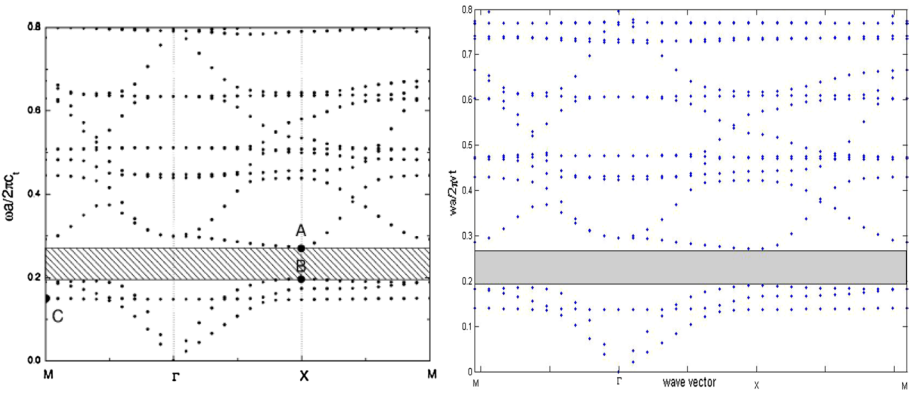

Fig. 3 Comparison between our results (left) and the result (right) published by Zhang et al. (2003)

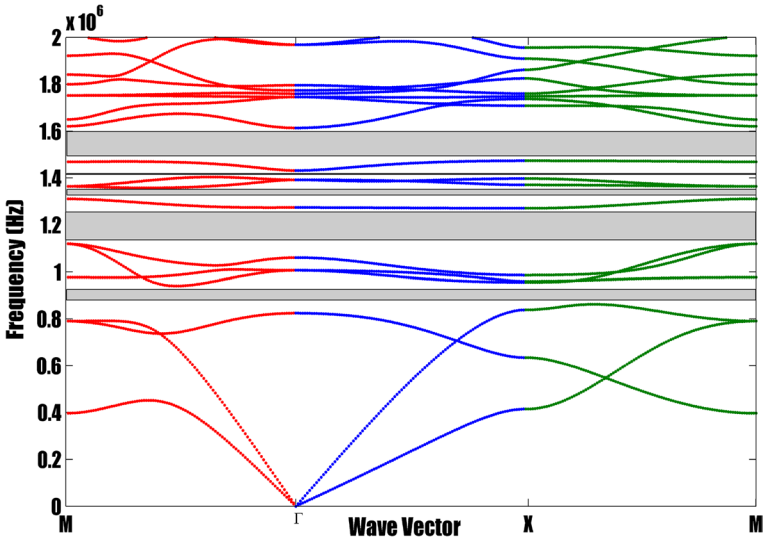

Fig. 4 The elastic wave band structure of carbon cylinders arranged in a square lattice in epoxy resin matrix the filling fraction is 0.72. The frequency gap range is marked by coloured area (band gap is represented by the grey colour)

The triangular band structure in Fig. 6 shows 3 absolute gaps in the frequency range: 0.8 MHz $< f_q <$ 1.85 MHz The largest gap appears between the 3rd and the 5th bands and has a width of $\Delta f_q = 0.61$ MHz, its gap-midgap ratio is $\Delta f_q / f_{qg} = 0.59$.

We can see that there are no gaps at low frequencies for a band structure obtained by the two lattices, those gaps depend on the periodicity called the Bragg gap. In fact, such construction of phononic structures in the audible frequency range based on the Bragg periodicity mechanism is very large and so very large dimensions are used. For example, to obtain a gap in the range of 1 kHz we must use a = 2 m and R = 0.8 m according to the Bragg theory.

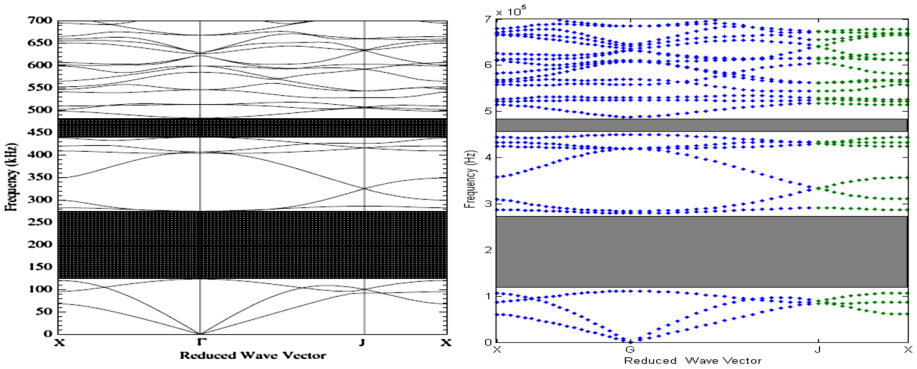

Fig. 5 Comparison between our theoretical work and ref [6]which is compared to an experimental result

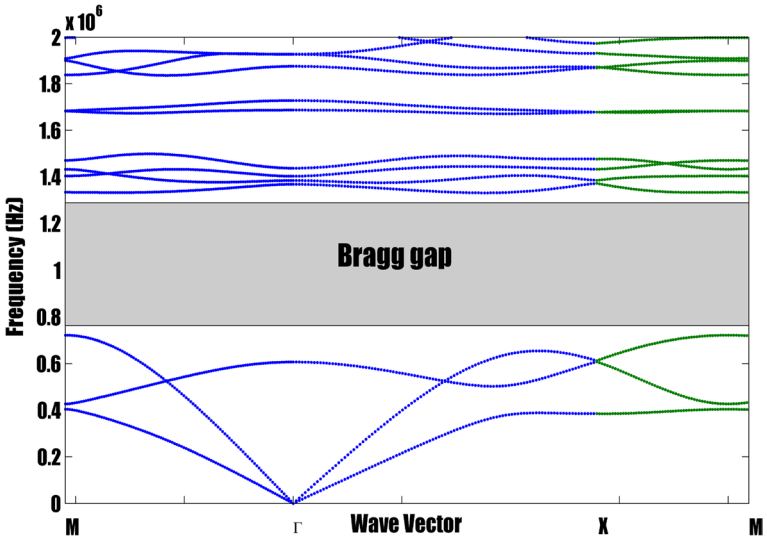

Fig. 6 The elastic wave band structure of carbon cylinders arranged in a triangular lattice of epoxy resin matrix with a filling fraction of 0.72

3.1.3 Effect of the filling fraction

Before studying the LR structure, we discuss the effect of the filling fraction Fig. 7 on the band gap of a carbon rod embedded periodically in the square background with a lattice parameter a = 3 mm.

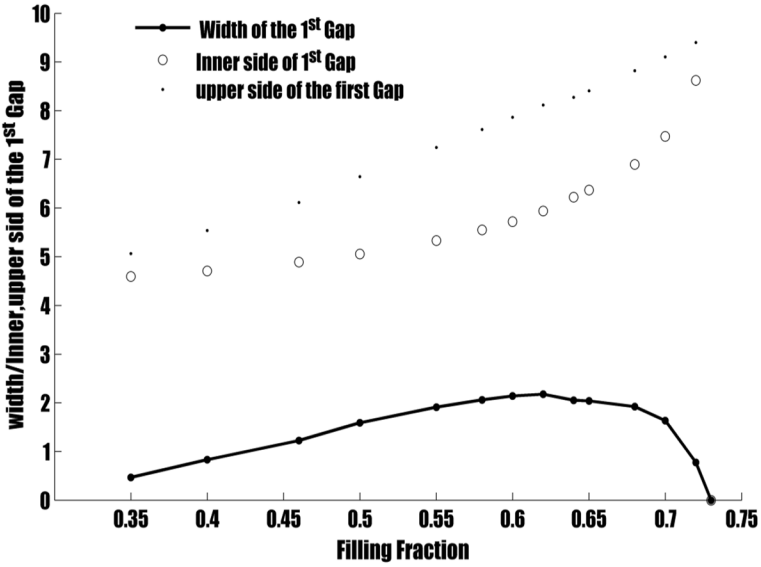

Fig. 7 First band gap width varying with the filling fraction

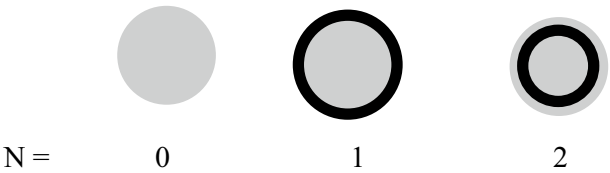

Fig. 8 Carbon rods coated with N layers

3.2 Locally resonant phononic crystal

We use N Fig. 8 as the number of layers that cover the carbon core and study two cases, where N = 1 and 2 respectively, for a matrix in contact with the carbon and the polymer. We obtain the coating structure using a superposition procedure.

The physical parameters of the three components are selected to satisfy the relation that the coating layer is softer than the matrix and the core (the part to be coated) to form the localized resonance structure.

3.2.1 Square lattice (N = 1)

Figure 9 shows results for the case in which we coat every rod of carbon with 0.48 mm of silicon rubber keeping the same outer radius. The band gap is shifted to lower frequency range. We see two absolute gaps with the first gap appearing between the 3rd and the 4th bands with a width $\Delta f_q = 2.8470$ kHz, with upper and lower edges are 8.8490 kHz and 6 kHz and a gap-midgap ratio is $\Delta f_q / f_{qg} = 0.3834$. The second gap appears between the 6th and the 7th bands with a width $\Delta f_q = 0.76$ kHz, with upper and

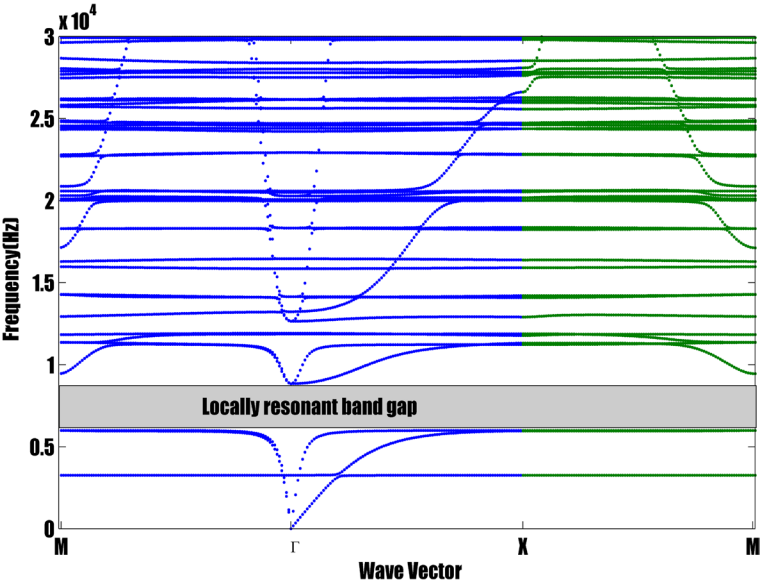

Fig. 9 The elastic wave band structure of coating carbon cylinders arranged in square epoxy resin lattice. The filling fraction of coating cylinders is 0.72, with a thickness of polymer = 0.48 mm

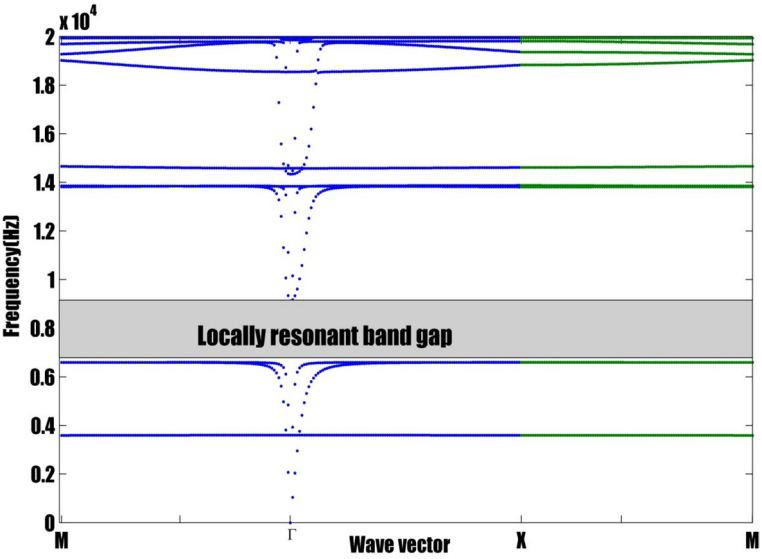

Fig. 10 The elastic wave band structure of coating carbon cylinders arranged in a square lattice of epoxy resin background when the core is coated by two shells. The filling fraction of coating cylinders is 0.72. With a polymer thickness = 0.48 mm and carbon layer thickness = 0.1 mm

lower edges are 12.65 kHz and 11.89 kHz its gap-midgap ratio is $\Delta f_q/f_{qg}=0.0619$, we see a partial gap along the XM direction.

3.2.2 Square lattice (N = 2)

If we add a second layer (0.1 mm of carbon) keeping the same thickness of polymer (0.48 mm) leading to all changes to be related on the inner radius of carbon rod. We see two absolute gaps (Fig. 10), the largest appears between the 3rd and the 4th bands with a width $\Delta f_q=2.52$ kHz, the upper and lower edges are at 9.12 kHz and 6.59 kHz. Its gap-mid-gap ratio is $\Delta f_q/f_{qg}=0.321$. The second Gap appears between the 6th and the 7th bands with a width $\Delta f_q=0.49$ kHz, with upper and lower edges at 14.36 kHz and 13.87 kHz and a gap-midgap ratio is $\Delta f_q/f_{qg}=0.034$. We can also see many partial gaps along the XM direction.

By comparing the band structures of Figs. 9 and 10, we see that for a rod coated with two layers, the number of modes is much less than those obtained by the rods coated with one layer, so those modes are confined in the Carbone layer. For the carbon rod coated with hard and heavy materials many modes get closer to create an expanded scale near the Γ Point.

3.2.3 Square lattice (N > 2)

If we add three layers (silicon rubber-carbon-silicon rubber) to the carbon rod keeping the same filling fraction f = 0.75. The complete gap appears between the 3rd and the 4th bands with a width of ΔF = 2.639 kHz, the upper and the lower edges are at 8.678 kHz and 6.039 kHz. Its gap-mid gap ratio is ΔF/Fg = 0.2543. If we compared Fig. 11 with Figs. 9 and

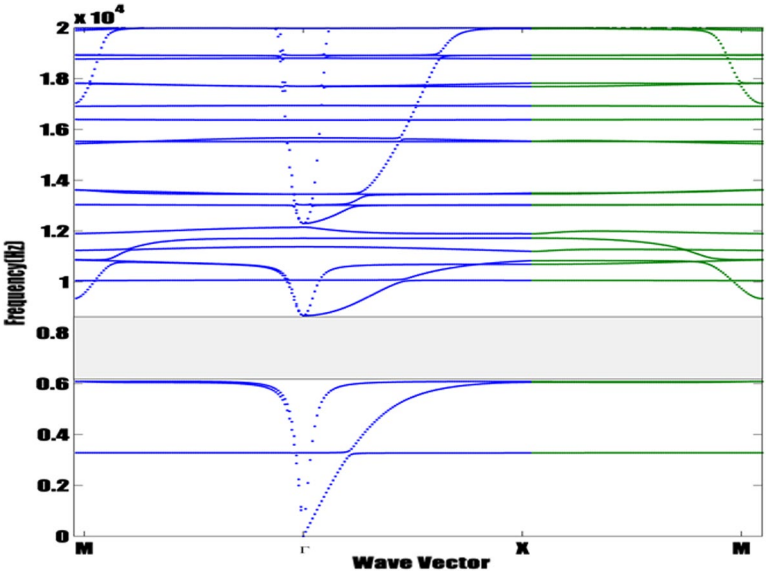

Fig. 11 The elastic wave band structure of coating carbon cylinders arranged in a square lattice of epoxy resin background when the core is coated by three shells. The filling fraction of coating cylinders is 0.72

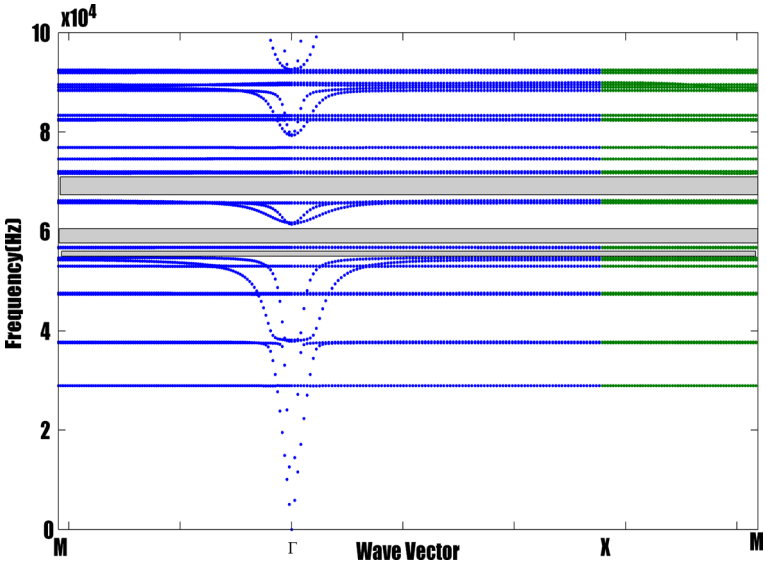

Fig. 12 The elastic wave band structure of coating carbon cylinders embedded in a triangular epoxy resin lattice. The filling fraction of coating cylinders is 0.72, with a polymer thickness = 0.48 mm

10, it can be seen that the first gap (Fig. 11) is larger and shifted to lower frequencies meanwhile the second gap around 13 kHz disappear.

3.2.4 Triangular lattice (N = 1)

In this section we study the effect of LRPC with a triangular lattice with the same parameters used in a square lattice. On comparing the band structures obtained for both, a square (Fig. 9) and a triangular (Fig. 12) lattice, we see that for the triangular lattice, there are more number of modes contrary to the band structure of a square lattice. We obtain many modes and gaps for the triangular lattice; however, we focus our study on frequencies lower than 10 kHz. We can notice that the width of the complete gap obtained by a triangular lattice has a small width with a position shifted to lower frequencies.

3.2.5 Triangular lattice (N = 2)

We can see first that by adding 0.1 mm of carbon layer (Fig. 13) many modes disappear and the others shift to lower frequency and get closer near the Γ point. This behavior was observed in square lattice. Second, the first band gap is larger than the one obtained by carbon rod coated with one layer, and its migap move from 58 to 8 kHz.

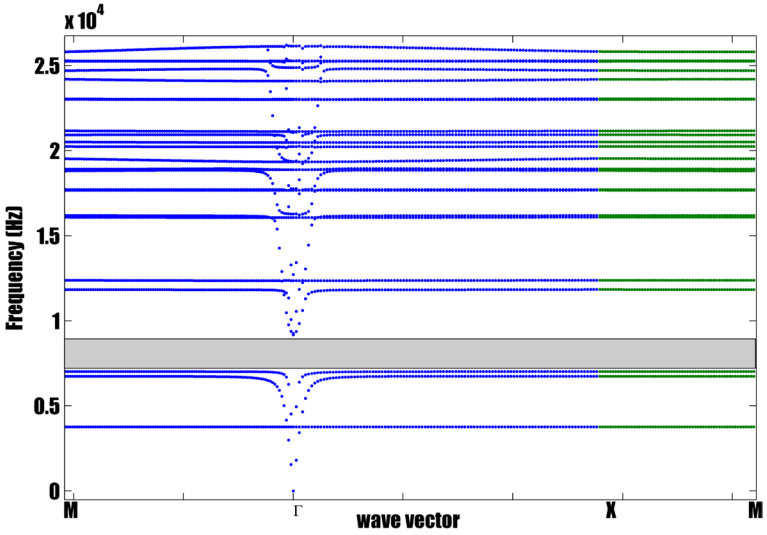

Fig. 13 The elastic wave band structure of coating carbon cylinders embedded in triangular epoxy resin lattice. The filling fraction of coating cylinders is 0.72, with a polymer thickness = 0.48 mm and carbon thickness = 0.1 mm

4 Conclusion

In summary, we investigated the locally resonant phononic band gaps of a 2D phononic crystal composed of carbon rods coated with one, then two layers immersed in a soft matrix of square and triangular lattices. The plane wave expansion method is used assuming an infinite medium, considering a structure with a lattice parameter of the order of a few millimeters. For inclusion coated with one layer and arranged in square and triangular lattice we obtained a LR band localized in the range of sonic frequency. For coated rods with two layers arranged in triangular lattice the band gap is larger and lower than those obtained by rod coated in one layer. Also many narrow pass band were found, which has potential applications for acoustic filtering of noise and transport in phononic metamaterials.

References

Achaoui, Y., Khelif, A., Benchabane, S., Robert, L., Laude, V.: Experimental observation of locally-resonant and Bragg band gaps for surface guided waves in a phononic crystal of pillars. Phys. Rev. B **83**(10), 104201 (2011)

Bria, D., Assouar, M.B., Oudich, M., Pennec, Y., Vasseur, J., Djafari-Rouhani, B.: Opening of simultaneous photonic and phononic band gap in two-dimensional square lattice periodic structure. J. Appl. Phys. **109**(1), 014507 (2011)

De Espinosa, F.M., Jimenez, E., Torres, M.: Ultrasonic band gap in a periodic two-dimensional composite. Phys. Rev. Lett. **80**(6), 1208 (1998)

Herring, C.: A new method for calculating wave functions in crystals. Phys. Rev. **57**(12), 1169 (1940)

Hou, Z., Assouar, B.M.: Numerical investigation of the propagation of elastic wave modes in a one-dimensional phononic crystal plate coated on a uniform substrate. J. Phys. D Appl. Phys. **42**(8), 085103 (2009)

Huang, Z.G., Wu, T.T.: Analysis of wave propagation in phononic crystals with channel using the plane-wave expansion and supercell techniques. In: IEEE Ultrasonics Symposium, 2005. vol. 1, pp. 77–80. IEEE, New York (2005)
Jiang, S., Hu, H., Laude, V.: Low-frequency band gap in cross-like holey phononic crystal strip. J. Phys. D Appl. Phys. **51**(4), 045601 (2018)
Khelif, A., Adibi, A.: Phononic Crystals. Springer, Berlin (2015)
Khelif, A., Achaoui, Y., Benchabane, S., Laude, V., Aoubiza, B.: Locally resonant surface acoustic wave band gaps in a two-dimensional phononic crystal of pillars on a surface. Phys. Rev. B **81**(21), 214303 (2010)
Kushwaha, M.S.: Band gap engineering in phononic crystals. Recent Res. Dev. Appl. Phys. **2**, 743–855 (1999)
Kushwaha, M.S., Halevi, P., Dobrzynski, L., Djafari-Rouhani, B.: Acoustic band structure of periodic elastic composites. Phys. Rev. Lett. **71**(13), 2022 (1993)
Larabi, H., Pennec, Y., Djafari-Rouhani, B., Vasseur, J.O.: Locally resonant phononic crystals with multilayers cylindrical inclusions. J. Phys: Conf. Ser. **92**(1), 012112 (2007)
Li, Y.F., Meng, F., Li, S., Jia, B., Zhou, S., Huang, X.: Designing broad phononic band gaps for in-plane modes. Phys. Lett. A **382**(10), 679–684 (2018)
Liu, Z., Zhang, X., Mao, Y., Zhu, Y.Y., Yang, Z., Chan, C.T., Sheng, P.: Locally resonant sonic materials. Science **289**(5485), 1734–1736 (2000)
Meade, R.D., Brommer, K.D., Rappe, A.M., Joannopoulos, J.D.: Existence of a photonic band gap in two dimensions. Appl. Phys. Lett. **61**(4), 495–497 (1992)
Pennec, Y., Vasseur, J.O., Djafari-Rouhani, B., Dobrzyński, L., Deymier, P.A.: Two-dimensional phononic crystals: examples and applications. Surf. Sci. Rep. **65**(8), 229–291 (2010)
Plihal, M., Maradudin, A.A.: Photonic band structure of two-dimensional systems: the triangular lattice. Phys. Rev. B **44**(16), 8565 (1991)
Sigalas, M.M.: Elastic wave band gaps and defect states in two-dimensional composites. J. Acoust. Soc. Am. **101**(3), 1256–1261 (1997)
Sigalas, M.M., Economou, E.N.: Solid State Commun. **86**, 141 (1993)
Sigalas, M.M., Economou, E.N.: Elastic waves in plates with periodically placed inclusions. J. Appl. Phys. **75**(6), 2845–2850 (1994)
Sigalas, M.M., Economou, E.N.: Attenuation of multiple-scattered sound. EPL (Europhys. Lett.) **36**(4), 241 (1996)
Vasseur, J.O., Djafari-Rouhani, B., Dobrzynski, L., Kushwaha, M.S., Halevi, P.: Complete acoustic band gaps in periodic fibre reinforced composite materials: the carbon/epoxy composite and some metallic systems. J. Phys.: Condens. Matter **6**(42), 8759 (1994)
Vasseur, J.O., Deymier, P.A., Frantziskonis, G., Hong, G., Djafari-Rouhani, B., Dobrzynski, L.: Experimental evidence for the existence of absolute acoustic band gaps in two-dimensional periodic composite media. J. Phys.: Condens. Matter **10**(27), 6051 (1998)
Vasseur, J.O., Deymier, P.A., Djafari-Rouhani, B., Pennec, Y., Hladky-Hennion, A.C.: Absolute forbidden bands and waveguiding in two-dimensional phononic crystal plates. Phys. Rev. B **77**(8), 085415 (2008)
Zhang, X., Liu, Y., Wu, F., Liu, Z.: Large two-dimensional band gaps in three-component phononic crystals. Phys. Lett. A **317**(1–2), 144–149 (2003)